Extraction of Lignin from a Coproduct of the Cellulosic Ethanol Industry and Its Thermal Characterization

Vida Poursorkhabi,[a,b] Manjusri Misra,[a,b,*] and Amar K. Mohanty [a,b]

Lignin was extracted from the solid coproduct of a lignocellulosic ethanol production by a solid-liquid extraction method using N,N-dimethyl formamide. This coproduct was the residue of a steam explosion pretreatment followed by enzymatic hydrolysis process. The coproduct was used as received and also after washing. Lignin content of the solid coproduct was reduced from 63% to 43% after lignin extraction. Fourier transform infrared spectroscopy (FTIR), molecular weight measurement (GPC), and elemental analysis provided information about the chemical structure and molecular weight of the fractions. The extracted lignin had lower molecular weight (~ 5000 Da.) and higher carbon content (63%) compared to the residue of extraction (M_w ≈ 8000 Da. and carbon % = 48%). Thermal stability measurements of the samples by thermogravimetry (TGA) showed that the extracted lignin had the highest carbon residue. Effects of different heating cycles on the glass transition temperature (T_g) were measured. The T_g of the soluble fraction was lower than that of the coproduct. Results of the X-ray diffraction (XRD) showed the crystalline structure of cellulose in both the coproduct and the solid residue after extraction. This extraction and material characterization is helpful for liquid processes such as solution spinning or electrospinning. The thermal properties can be used for optimization of heat treatment processes such as carbonization.

Keywords: Solid-liquid extraction of lignin; Enzymatic hydrolysis coproduct; Glass transition temperature; Thermal stability; Steam explosion lignin

*Contact information: a: School of Engineering, Thornbrough Building, University of Guelph, Guelph, N1G 2W1, Ontario, Canada; b: Bioproducts Discovery and Development Centre, Department of Plant Agriculture, Crop Science Building, University of Guelph, Guelph, N1G 2W1, Ontario, Canada; *Corresponding author: mmisra@uoguelph.ca*

INTRODUCTION

Environmental issues, such as climate change and waste management of traditional plastics, have inspired ideas to replace petroleum-based materials with renewable resource–based and natural products. The addition of bioethanol to engine fuels is one of the attempts to reduce greenhouse gas emissions (FitzPatrick *et al.* 2010; Sims *et al.* 2010). First-generation bioethanol plants were designed to convert sugar from food crops such as cereals, sugar crops, and oil seeds to ethanol. To overcome challenges and issues associated with grain-based ethanol, a cellulosic ethanol process has been developed.

Production of ethanol from cellulosic material involves three main steps: (1) pretreatment of lignocellulosic material to separate lignin from cellulose and hemicellulose and make them accessible to the hydrolyzing agents, (2) hydrolysis of cellulose and hemicellulose, and (3) fermentation of sugars by microorganisms, followed by distillation to isolate the alcohol (Sims *et al.* 2010). Several physical, chemical,

biological, and physico–chemical methods of pretreatment are available to break down the structure of the lignocellulosic material and to separate lignin from carbohydrates (Alvira *et al.* 2010; Kumar *et al.* 2009). The outcome of this step is a mixture of cellulose, hemicellulose, broken-down and low molecular weight lignin (Ramos *et al.* 1999; Shevchenko *et al.* 1999), lignin–carbohydrate complexes, residues of inorganic materials that entered the process with the biomass, and other chemicals produced during the process such as furans and acids (Kumar *et al.* 2013). Usually, the same mixture coming out of the pretreatment stage is directly sent to the hydrolysis reactor. The reaction can be either acid hydrolysis or enzymatic hydrolysis. The carbohydrates are converted to sugars, and the part that is not hydrolyzed makes up the coproduct of the process (Kumar *et al.* 2009; Lynd 1996; Taherzadeh and Karimi 2007).

Cellulosic ethanol, or second-generation ethanol production, has been extensively studied to decrease its cost and increase profitability. One of the several methods available to increase the profitability of this process is to use the coproducts in valuable applications (Doherty *et al.* 2011; Gellerstedt *et al.* 2010). The major constituent of cellulosic ethanol coproduct is lignin. Considering the current rate of production and increasing demand for ethanol fuel, a great amount of this material will be produced annually. Currently, most of the coproducts are disposed of in the landfill or burned in-plant to produce electricity. Just a small amount is converted to chemicals or used in phenolic resins (Hatakeyama *et al.* 2010; Holladay *et al.* 2007; Kumar *et al.* 2009; Suhas *et al.* 2007). One of the obstacles of utilizing the bioethanol coproduct is its impurities and the need for separating lignin (Lora and Glasser 2002).

One of the proposed applications for lignin is its spinning and further carbonization (Gellerstedt *et al.* 2010; Suhas *et al.* 2007). Melt spinning and electrospinning of lignin have been studied (Kadla *et al.* 2002; Kubo and Kadla 2005). One of the disadvantages and issues with the melt spinning of lignin is its thermal degradation at the high processing temperatures that are required for melting and extruding the blended polymers with lignin (Kubo and Kadla 2005). In contrast, electrospinning is performed at room temperature and only requires solubility of the materials. Although electrospinning of commercially available lignins have been reported (Dallmeyer *et al.* 2010), solution preparation for electrospinning of lignin from an impure industrial coproduct needs an extra step of lignin extraction. A solid-liquid extraction method merges the lignin extraction step with the solution preparation. Several solvents have been used for lignin extraction from the bioethanol coproduct, but not all of these solvents are good solvents for the electrospinning (Guo *et al.* 2013). Knowing that N,N-dimethyl-formamide (DMF) is a good solvent for electrospinning, it was used to extract the lignin. Since the extracted material in the solution will be the structural material of the fiber upon the spinning, its properties such as molecular weight, purity, and thermal properties affect the fiber properties as well as the consequent processing conditions such as carbonization.

In this study, the coproducts of a cellulosic ethanol process were used as the source of lignin. In this process, subsequent to steam explosion pretreatment, the material was enzymatically hydrolyzed and sent to a solid–liquid separation unit. The liquid phase was sent to the fermentation unit and the solid residue was defined as the coproduct. The structural composition and properties of the coproduct were determined by the feedstock as well as by the process parameters that are usually not available to the downstream processors who aim to use the coproduct. In this study, the received coproduct (which will be referred to as hydrolysis lignin), was dried and water-washed prior to

fractionation. N,N-dimethyl formamide (DMF) was selected from an array of organic solvents to selectively extract lignin from this coproduct. As a result of extraction, the coproduct was fractionated into a soluble fraction, which was rich in lignin and an insoluble residue, which was cellulose-rich. To determine the structure of each fraction, analytical techniques such as Fourier transform infrared spectroscopy (FTIR), elemental analysis, and gel permeation chromatography (GPC) were used. By means of thermal analysis, the transition temperatures and thermal stability of each fraction were determined. Crystallinity of the samples was studied by X-ray diffraction.

EXPERIMENTAL

Materials

Pre-treated poplar hydrolysate solid residue was used as hydrolysis lignin. It was the solid residue of enzymatic hydrolysis of poplar and was provided by the bioethanol plant Mascoma (Canada). The received coproduct had 55 to 57 wt% dry content, and it was frozen. Ash content was measured following the NREL method (Sluiter *et al.* 2005), and it was 2.13%. The hydrolysis lignin was dried in an oven at 105 °C for 12 h. The material was ground in a planetary ball mill (Retsch PM100) at 200 rpm for 24 h. This rate is low enough to preserve the crystallinity of cellulose (Paes *et al.* 2010), which might be present in the sample as an impurity. The milled lignin was sieved to obtain two samples with different particle size. One sample passed the 1 mm sieve, and the other sample passed 150 μm sieve and so had finer particles.

This coproduct was directly received after hydrolysis without further washing. Therefore small sugar molecules and soluble oligosaccharides were available in this sample. Furthermore, based on the material data sheet provided by the company, this sample has other types of impurities such as sodium or potassium salts, enzymes such as industrial cellulases, and lignin-derived phenolic acids. To study the effect of washing the sample and removing the soluble impurities, in addition to testing the dried hydrolysis lignin, a water-washed sample of hydrolysis lignin was also studied. For washing, 2 g of dried and milled hydrolysis lignin was stirred in 200 mL distilled water at 60 °C for 2 h. Then, it was filtered, rinsed with excess water, and dried in an oven at 105 °C for 12 h. The yield from the washing was 93 wt%.

Cellulose was also tested in the same way as the lignin fractions to help explain the behavior of the hydrolysis lignin and the fractions that contained cellulose. Micro crystalline cellulose powder was supplied by MP Biomedicals. Organic solvents used for the solubility testing and extraction were purchased as follows: N,N-dimethyl formamide (DMF) and furfuryl alcohol from Acros, tetrahydrofuran (THF) and chloroform from Fisher Scientific.

Solubility Studies (solid-liquid extraction)

Solubility of hydrolysis lignin was examined in N,N-dimethyl formamide (DMF), furfuryl alcohol, tetrahydrofuran (THF), and chloroform. A solution of 1 wt/vol% of hydrolysis lignin in each solvent was refluxed for 24 h. After separating the insoluble residue by filtration, distilled water was added to the solution to precipitate the dissolved polymer. However, if there are some dissolved carbohydrates, they will stay in the solution and will not precipitate with lignin. The soluble and insoluble fractions were

dried in a vacuum oven at 140 °C for 21 h. Completion of drying was confirmed by observed removal of solvent peaks in FTIR spectra of samples.

Compositional Analysis

Moisture analysis

Moisture content of the samples was measured by a Denver Instrument–IR 35 moisture analyser. It kept the sample at 105 °C until the weight became constant for a certain amount of time, and then reported the weight percentage of moisture.

Lignin and total carbohydrate content measurements

The lignin content of the washed hydrolysis lignin, soluble fraction, and insoluble residue in DMF was measured by the NREL method for "Determination of structural carbohydrates and lignin in biomass" (NREL/TP-510-42618, Revised 2010) (Meunier-Goddik *et al.* 1999; Sluiter *et al.* 2008; Thammasouk *et al.* 1997). Briefly, the sample was hydrolyzed with sulfuric acid. Then the amount of acid-soluble lignin was calculated from the UV absorptivity of the solution at 240 nm (Varian UV-Visible Spectrometer–CARY 300 Bio was used for this measurement). The acid-insoluble lignin was calculated as weight of the insoluble material minus the weight of its ash content. The percentage of lignin in the sample was the sum of acid-soluble and acid-insoluble lignins. This analysis was repeated four times and the average was reported. The hydrolysis lignin samples were selected from both the fine particles passed through 150 μm and the larger particles with a size near 1 mm.

The sum of cellulose, hemicellulose, and lignin content (known as neutral detergent fiber or NDF) was measured following AOAC method 2002.04 by AgriFood Laboratories, Guelph, Ontario, Canada. For washed hydrolysis lignin and the insoluble residue in DMF, the carbohydrate content was calculated by deducting the lignin content from the NDF.

Elemental analysis

A Thermo-scientific Elemental Analyzer–Flash 2000 was used to measure the carbon, nitrogen, and oxygen content of the washed hydrolysis lignin, soluble and insoluble fractions in DMF. For one of the samples, acid soluble and acid insoluble lignin were dried and tested to measure the nitrogen content.

Molecular weight measurement

Molecular weight of the washed hydrolysis lignin, and its soluble and insoluble fractions in DMF, were measured by gel permeation chromatography (GPC) using three Styragel HR columns (Waters), HR 0.5, 1, 2 in series and a refractive index detector. Tetrahydrofuran was used as the mobile phase with a flow rate of 0.6 mL/min. Standard solutions of polystyrene with molecular weights of 1540, 2858, 5230, 14830, and 19280 Da were used for calibration. Samples were acetylated prior to the analysis. For acetylation, 0.5 g of each sample was dissolved in 6 mL pyridine/acetic anhydride (1:1 volume ratio) and stirred for one week. Then the acetylated material was precipitated by adding the solution dropwise into 100 mL ice-water containing 1 mL hydrochloric acid (HCl). Then the precipitated material was filtered and dried (Pan *et al.* 2006).

Fourier Transform Infrared Spectroscopy (FTIR)

Fourier transform infrared (FTIR) spectroscopy was performed on a Thermo Scientific–Nicolet 6700 FTIR spectrometer in attenuated total reflection infrared (ATR-IR) mode. The spectra were recorded in the wavenumber range of 4000 to 500 cm^{-1} in the transmittance mode at a resolution of 2 cm^{-1}, with 36 scans per sample.

Thermal Analysis

Thermal analysis experiments were replicated three times, and the results were reproducible.

Thermogravimetry (TGA) experiments were performed with TA Instruments–TGA Q500 equipment. Samples were heated from 25 °C to 800 °C, at a heating rate of 10 °C/min in a nitrogen atmosphere.

Differential scanning calorimetry (DSC) was done with TA Instruments–DSC Q200 equipment. An amount 5 to 6 mg of each sample was heated in closed aluminum pans, under a nitrogen atmosphere (flow rate: 50 mL min^{-1}). The T_g of lignin depends on its origin, characterization, and thermal history (Hatakeyama *et al.* 1982). Therefore, three different thermal treatments were applied to clear the thermal history and to study the effect of time and temperature of the thermal treatment on the DSC results. As shown in Fig. 1, treatment I was a temperature increase from −20 °C to 90 °C at a rate of 10 °C/min followed by cooling to −20 °C at a rate of 20 °C/min. Then there was a heat/cool/heat cycle from −20 °C to 250 °C with a heating rate of 5 °C/min and a cooling rate of 20 °C/min. Treatment II was the same as Treatment I, except that at the end of the first heating to 90 °C, the sample was kept isothermal at 90 °C for 20 min. Treatment III was a heat/cool/heat cycle with a lower temperature of −20 °C and an upper temperature of 200 °C for the first heating, and 250 °C for the second heating. For heating to 200 °C and 250 °C, the heating rates were 10 °C/min and 5 °C/min, respectively. The cooling rate was 20 °C/min. The T_g values were measured from the second heating.

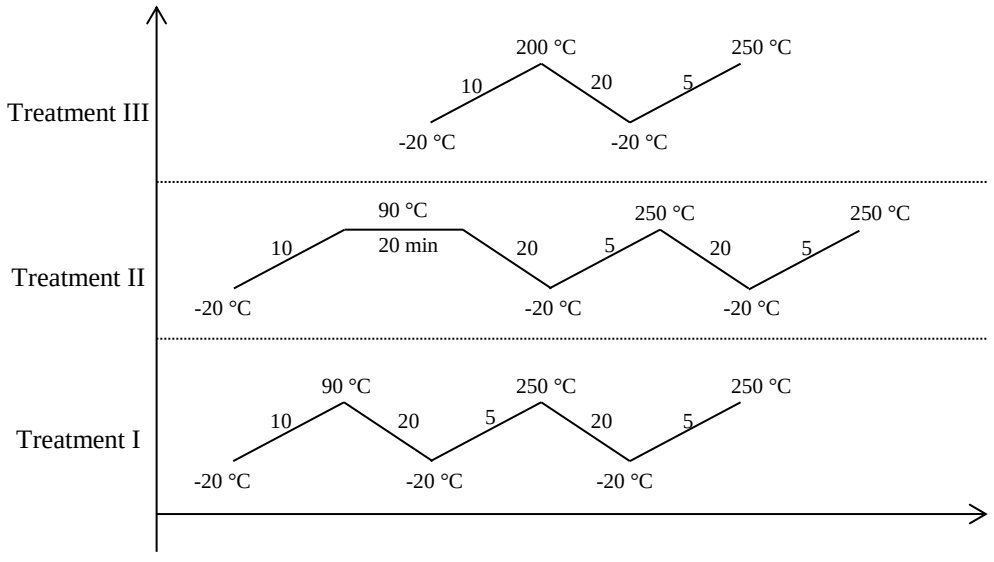

Fig. 1. Heat treatment cycles for DSC experiments. The numbers written on the lines are the heating rates in °C/min.

Temperature-modulated DSC experiments (TMDSC) were performed on the same DSC equipment at a heating rate of 2 °C/min, with a scanning temperature in the range of −20 °C to 250 °C. The amplitude and frequency of pulses were 2 °C and 60 s, respectively. Since T_g of lignin is dependent on its water content (Bouajila *et al.* 2006), the average moisture content of samples was measured before the experiments, and was kept approximately constant for all of the samples. Therefore, the effect of water was the same for all the samples.

X-ray Diffraction (XRD)

X-ray diffraction (XRD) patterns were measured in a STOE two-circle goniometer using Cu characteristic radiation from an ENRAF NONIUS FR 571 rotating anode generator. The X-rays were detected with a MOXTEK energy-sensitive Si detector connected to single channel analyzers that selected photons corresponding to the Cu Kalfa radiation (Lambda = 1.54178 A).

RESULTS AND DISCUSSION

A schematic summary of the experimental procedure for the lignin extraction and the results are shown in Fig. 2.

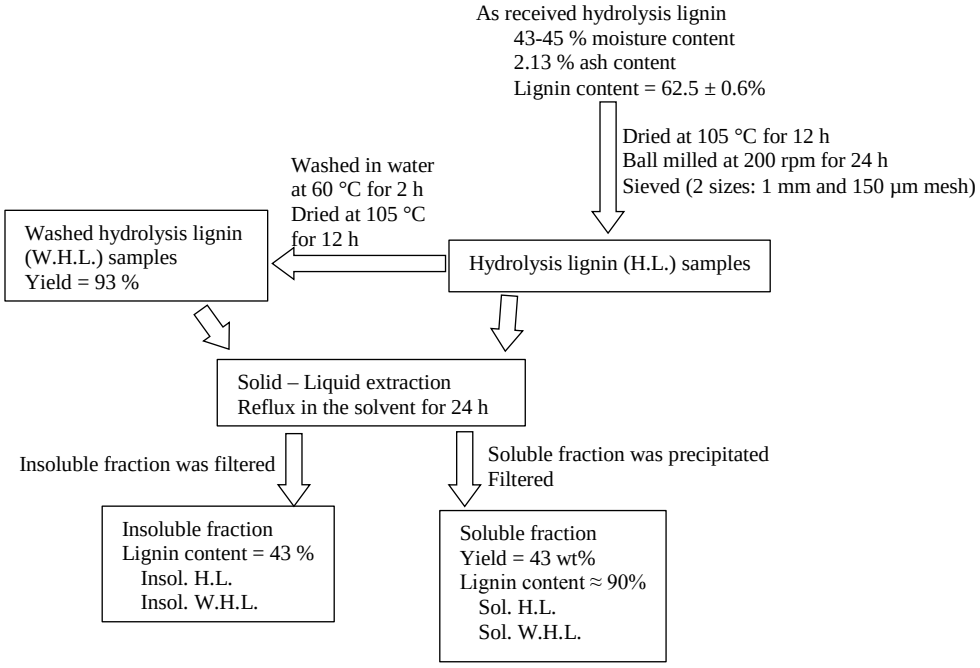

Fig. 2. The experimental procedure for solid-liquid extraction of hydrolysis lignin

Solubility Study

The main purpose of the liquid extraction in this study was to utilize a simple method to isolate lignin from various impurities that are present in the hydrolysis lignin. These impurities are residues that were created or added during pretreatment and hydrolysis steps.

In order to find a suitably selective solvent for a specific compound, established theoretical methods require the knowledge of functional groups available in the structure

of the material. Native lignin has a complex structure that has to be broken down at several points, during the pretreatment, to release the cellulose. Based on the pretreatment technique, the chemical degradation occurs with different mechanisms, resulting in isolated lignins with different functionalities (Guigo *et al.* 2009; Lora and Glasser 2002). Therefore, the application of theoretical methods requires several estimations or the determination of the lignin chemical structure by complicated chemical analysis methods. In this study, the solubility data that are available for kraft lignin (Hansen 2000) and also other reports regarding good solvents for lignin (Skrebets and Bogolitsyn 2009) were used to find candidate solvents to extract lignin from hydrolysis lignin. The percentage of solubility of the coproduct in DMF, furfuryl alcohol, THF, and chloroform, was 43, 21, 31, and 21 wt%, respectively. Based on these results, the highest amount of solubility occurred in DMF.

In the following sections, the results of analysis of DMF soluble and insoluble fractions are discussed.

Compositional Analysis

Moisture content analysis showed that the as-received hydrolysis lignin, before drying, had a high average water content of 53%. After the hydrolysis lignin was dried and maintained at ambient conditions, the average equilibrium moisture was 2%.

The average lignin content of four hydrolysis lignin samples with different particle size was 62.5 ± 0.6%. The small standard deviation shows the uniformity of the composition of the material within the smaller and larger particles after milling. The amount of lignin remaining in the insoluble residue in DMF was 43 ± 1.9% of the insoluble material. This insoluble lignin is either attached to cellulose or is a high molecular weight insoluble material. The lignin content of the soluble material in DMF as calculated following the NREL method (NREL/TP-510-42618, Revised 2010) was 92.9 ± 0.4%. However, this value is an estimation of the true lignin content of the dissolved material. One of the impurities and sources of error in measuring lignin content of enzymatically hydrolyzed samples following the standard acid hydrolysis method (Sluiter *et al.* 2008) is the residual enzymes or proteins, which increase the weight of acid-insoluble lignin. The amount of residual enzymes can be estimated by multiplying the nitrogen percentage of samples by a conversion factor of 6.25 (Mansouri and Salvadó 2006). Measurements of the percentage of nitrogen showed that these proteins mainly dissolved in the solvent (DMF) as contaminants of soluble fraction in DMF. Then they appeared in the acid-insoluble lignin and caused an increase in the weight. Therefore, the total weight of lignin in the soluble fraction of hydrolysis lignin is overestimated. The elemental analysis results (Table 1) confirmed that a large amount of enzymes or proteins are dissolved in the solvent.

The results of the carbohydrate content measurement showed that hydrolysis lignin and the insoluble fraction had 39 and 46 wt% carbohydrate. The results of elemental analysis (Table 1) show the percentage of carbon, oxygen, and nitrogen in the three samples. Washing with water under the applied conditions of this study cannot remove the proteins and they dissolve in the DMF. The soluble fraction had higher carbon and lower oxygen percentages compared with the insoluble residue. This was due to the higher percentage of lignin in the solution and its rich carbon structure compared with the higher percentage of carbohydrates in the insoluble residue.

Table 1. Elemental Analysis Results of Hydrolysis Lignin, Soluble and Insoluble Fractions in DMF

	Carbon (%)	Oxygen (%)	Nitrogen (%)
Hydrolysis lignin	53 ± 0.94	47 ± 0.61	0.18 ± 0.01
Washed hydrolysis lignin	52 ± 0.19	46 ± 0.61	0.18 ± 0.02
Soluble in DMF	63 ± 0.76	32 ± 0.93	1.98 ± 0.03
Insoluble in DMF	48 ± 0.28	50 ± 0.46	0.04 ± 0.07

Results of GPC are summarized in Table 2. After acetylation, the soluble fraction was completely soluble in THF, but the insoluble fraction and the coproduct before extraction were not completely soluble in THF. The solutions of the latter materials in THF were further filtered before injection in GPC. Therefore, the reported M.W. is not the real value, and it only shows the part which became soluble after acetylation. The DMF-insoluble fraction had the highest molecular weight compared with the soluble fraction and hydrolysis lignin. This can explain the low solubility of this fraction. The hydrolysis lignin was composed of high and low molecular weight lignin. The low molecular weight fraction was soluble in DMF while the high molecular weight remained in the insoluble residue.

Table 2. Molar Mass Results (M_n , M_w) and Polydispersity (M_w / M_n) of Washed Hydrolysis Lignin, Its Soluble and Insoluble Fractions in DMF

	M_n (Daltons)	M_w (Daltons)	M_w / M_n
Washed hydrolysis lignin	3129	5222	1.7
Soluble fraction in DMF	2697	5009	1.9
Insoluble fraction in DMF	3740	8324	2.2

FTIR Analysis

Figure 3 shows the FTIR spectra of hydrolysis lignin, soluble and insoluble fractions in DMF, and cellulose. Initially, all the figures appeared the same, which was due to the presence of lignin in both soluble and insoluble fractions. All the samples, except cellulose, had peaks at 1590, 1504, and 1421 cm^{-1}, due to the aromatic ring vibrations in lignin compounds (Boeriu *et al.* 2004; Li *et al.* 2012; Sahoo *et al.* 2011).

Comparison of the spectra shows that all the samples have a peak in the range of 3300 to 3500 cm^{-1}. Phenolic and aliphatic hydroxyl vibrations occur at 3400 cm^{-1} in lignins (Boeriu *et al.* 2004; Li *et al.* 2012) and at 3350 cm^{-1} in cellulose (Bjarnestad and Dahlman 2002). The peak of the hydrolysis lignin and insoluble residue is similar to cellulose while the peak for the soluble fraction is dominated by the behavior of lignin.

The next difference in the FTIR spectra occurs around 2900 cm^{-1}. Soluble material has a peak at 2930 cm^{-1} with a small shoulder at 2850 cm^{-1}. These peaks are due to CH vibrations in aromatic methoxyl groups and methyl groups in the side chains of lignin (Li *et al.* 2012; Lisperguer *et al.* 2009). Other samples have similar spectra to cellulose, which has a peak centered at 2900 cm^{-1} (Bjarnestad and Dahlman 2002). The band at 1710 cm^{-1} for the soluble sample is due to carbonyl/carboxyl bonds which are present in oxidized, solvent-extracted, and sulphur-free lignins (Boeriu *et al.* 2004). The

band at 1455 cm^{-1} in hydrolysis lignin and 1428 cm^{-1} in cellulose are due to CH_2 vibrations in both cellulose and lignin (Bodîrlâu and Teacâ 2009).

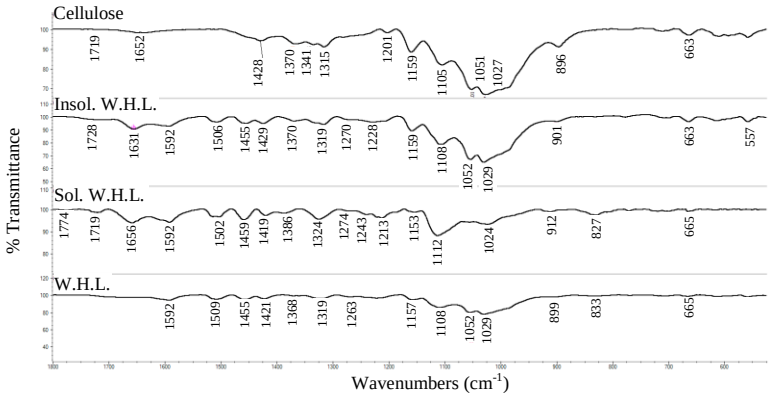

(a)

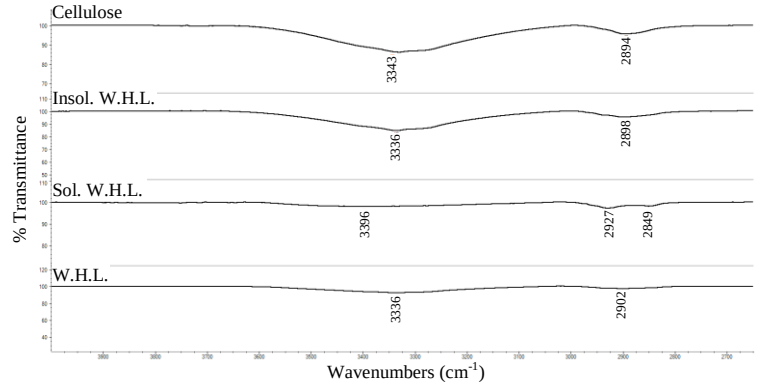

(b)

Fig. 3. FTIR spectra of hydrolysis lignin (H.L.), washed hydrolysis lignin (W.H.L.), insoluble fraction of hydrolysis lignin in DMF (Insol. H.L.), soluble fraction of hydrolysis lignin in DMF (Sol. H.L.), and cellulose (a) Spectra in the range of 1800-600 cm^{-1}, (b) Spectra in the range of 4000 – 2700 cm^{-1}

A peak at 1369 cm^{-1}, which appears for cellulose, hydrolysis lignin, and insoluble residue, is due to CH vibration in cellulose and hemicellulose (Ke *et al.* 2011).

The region below 1400 cm^{-1} provides information about structural units of lignin (Boeriu *et al.* 2004). The aromatic ring in syringyl and guaiacyl units results in absorption at 1324 cm^{-1} (Boeriu *et al.* 2004; Rutkowska *et al.* 2009) for soluble samples, while cellulose has a doublet at 1335 and 1316 cm^{-1} (Bodîrlâu and Teacâ 2009). For the insoluble sample and hydrolysis lignin, peaks of cellulose overlap the lignin peak at 1324 cm^{-1}, and so the superposition of peaks appears as a sharper peak and a shoulder.

Soluble sample and hydrolysis lignin exhibit characteristic peaks of guaiacyl units. These peaks appear at 1267, 1147, and 829 cm^{-1} due to ring and C=O stretching and CH vibrations (Boeriu *et al.* 2004; Lisperguer *et al.* 2009). The spectra of hydrolysis lignin and insoluble samples have weak peaks at 829 cm^{-1} and a band at 900 cm^{-1}, which can be attributed to C-O-C stretching in the cellulose spectrum (Bjarnestad and Dahlman 2002; Spiridon *et al.* 2011).

Cellulose has peaks at 1029 cm^{-1} because of CO stretching and at 1054 cm^{-1} due to axial deformations of C-O-C ether bonds (Ramos *et al.* 1999). For hydrolysis lignin and insoluble residue, these peaks overlap the peak for aromatic CH in plane deformation

of lignin at 1029 cm^{-1} and appear as a doublet (Ke *et al.* 2011). Only the soluble fraction shows a single peak in this region.

FTIR spectra confirm that lignin is available in both soluble and insoluble samples. The main component of the soluble sample is lignin, while the insoluble part is composed of both cellulose and lignin.

Thermogravimetric Analysis (TGA)

Thermal stability and degradation temperature of the samples were studied by TGA. The resulting graphs are shown in Fig. 4. Cellulose degradation is indicated in all the graphs for comparison. Table 3 reports temperature of degradation onset, which is the temperature that coincides with a 10% weight loss (T_{10}) of the sample, temperature at maximum rate of weight loss (T_{max}), which is the temperature at the maximum point in the derivative thermogravimetry (DTG) graph, and the weight percentage of the final residue, for each sample.

Table 3. Thermal Degradation Data of Hydrolysis Lignin and Its Soluble and Insoluble Fractions in DMF, Washed Hydrolysis Lignin, and Its Soluble and Insoluble Fractions in DMF, and Cellulose

	T_{10} [a] (°C)	T_{max} [b] (°C)	Residue (%)
Cellulose	307	336	0
Hydrolysis lignin	260	341	22
Soluble fraction	227	322	34
Insoluble fraction	287	353	17
Water-washed hydrolysis lignin	290	369	18
Soluble fraction	264	346	34
Insoluble fraction	290	355	14

[a] T_{10}: temperature at 10% weight loss.
[b] T_{max}: temperature at maximum point in DTG graph.

Figure 4a shows the effect of water-washing the hydrolysis lignin on its thermal degradation, and compares it with cellulose. After washing, an increase in both the onset and T_{max} was observed, which was due to the removal of small-molecule impurities from hydrolysis lignin. The TGA graph of cellulose indicates that compared with both lignins, its degradation started at a higher temperature (307 °C), but it degraded fast over a narrow temperature range, resulting in a lower T_{max} than the lignins. Figure 4b shows the results for cellulose, hydrolysis lignin, and its soluble and insoluble fractions in DMF. Values of T_{10} and T_{max} were highest for the insoluble residue, followed by the hydrolysis lignin and soluble fraction. High values for the insoluble fraction were due to the presence of cellulose. Even though hydrolysis lignin contained cellulose, the presence of low molecular weight molecules reduced the total percentage of cellulose in the sample, thereby resulting in the reduction of characteristic temperature values. Another explanation for reduced temperature measurements is the molecular weight of the insoluble residue. The insoluble fraction had higher molecular weight, which made it more resistant and thermally stable compared with the hydrolysis lignin and soluble fraction. In contrast, the soluble fraction had the lowest T_{10} and T_{max}. This sample had low molecular weight, and also the impurities that were dissolved in the solution started to degrade at a lower temperature, resulting in a wide degradation range.

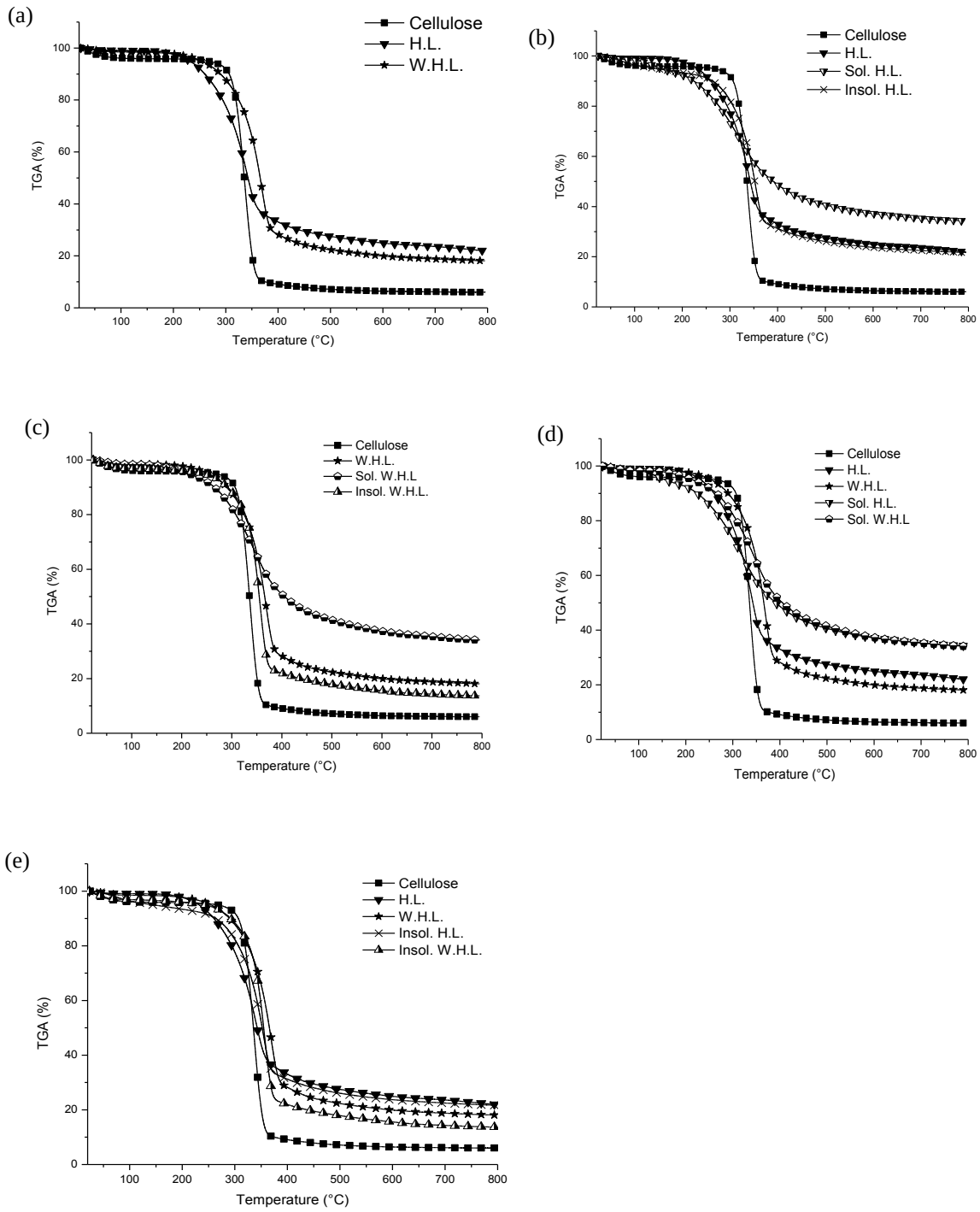

Fig. 4. TGA results of hydrolysis lignin (H.L.), soluble fraction of hydrolysis lignin in DMF (Sol. H.L.), insoluble fraction of hydrolysis lignin in DMF (Insol. H.L.), washed hydrolysis lignin (W.H.L.), DMF-soluble fraction of washed hydrolysis lignin (Sol. W.H.L.), DMF-insoluble fraction of washed hydrolysis lignin (Insol. W.H.L.), and cellulose. a) effect of washing hydrolysis lignin, b) comparison of soluble and insoluble fractions of hydrolysis lignin, c) comparison of soluble and insoluble fractions of washed hydrolysis lignin, d) comparison of soluble fraction of hydrolysis lignin and washed hydrolysis lignin, e) comparison of insoluble fraction of hydrolysis lignin and washed hydrolysis lignin.

Residue of the insoluble fraction was less than that of the hydrolysis lignin, and the residue of both the insoluble fraction and the hydrolysis lignin were lower than the residue of the soluble fraction. This is in agreement with the amount of carbohydrates in the samples; the higher percentage had the lower carbon residue.

Washing the hydrolysis lignin increased its thermal stability by removing the residual of hydrolyzed sugars. As a result, the TGA graph of washed hydrolysis lignin shifted to the right (Fig. 4c) compared with the unwashed sample. However, the relative positions of washed hydrolysis lignin and its soluble and insoluble fractions stayed the same as Fig. 4b. Figures 4d and 4e show the comparison between the soluble and insoluble fractions before and after washing. Both the soluble and insoluble fractions of washed hydrolysis lignin had higher stability (higher T_{10} and T_{max}) than the fractions of hydrolysis lignin. Furthermore, a detailed study of the TGA graph from the soluble fraction of hydrolysis lignin showed that there were several intermediate steps of weight loss before the main degradation occurred. After washing, these intermediate weight loss steps disappeared. Their disappearance confirms removal of the impurities of hydrolysis lignin dissolved in DMF which starts to degrade at lower temperatures than lignin. The increase in degradation temperatures of the insoluble residue after washing the hydrolysis lignin is less dramatic than the increase which occurs for the soluble fraction.

Results of TGA analysis were also used as a guide to select the upper temperature for thermal treatment with DSC. Based on the TGA results, degradation generally commenced after 200 to 250 °C. Therefore, these temperatures were used to select maximal heating temperatures during thermal treatment with DSC, to ensure that degradation did not occur. Also, TGA results revealed the effect of cellulose on the degradation behavior of lignin. Cellulose degrades across a narrow temperature range and has higher T_{max} than lignin, which has a broad degradation range and higher residue content. Increasing the percentage of either the cellulose or lignin component caused the blend to display thermal behavior resembling that of the respective component.

Differential Scanning Calorimetry (DSC) analysis

The effects of different thermal treatments at temperatures lower and higher than T_g are illustrated in Figs. 5 to 7. For the results of thermal treatment with Treatments I and II, only the graphs of the first and second heating following initial heating to 90 °C are shown here. For all the results, the cooling graph is omitted. Figure 5a shows the DSC of hydrolysis lignin and washed hydrolysis lignin treated at 200 °C (Treatment III). Both samples have a wide endothermic peak at 100 °C in the first heating due to dehydration of the sample. A similar endothermic peak was observed by Hatakeyama in the range of 77 to 177 °C for dioxane lignin (Hatakeyama *et al.* 1982). The broad peak of water evaporation in the first heating overlapped other thermal events in the range of 50 to 160 °C. In the second heating, the water evaporation peak disappeared, and T_g values were measured at 151 °C and 164 °C for the hydrolysis lignin and washed hydrolysis lignin, respectively. Washing the sample with water removed the sugar molecules and other degradation products and resulted in an increase in T_g. Figure 5b shows the effect of thermal treatment at 90 °C, which is below the T_g, and two different time intervals for isothermal heat treatments. Thermal treatment at temperatures below T_g caused the appearance of sub-T_g transition points (Hatakeyama *et al.* 2010). Three steps appeared for hydrolysis lignin after thermal treatment at 90 °C without holding the isothermal condition (H.L._90°C_0min). The DSC result of washed hydrolysis lignin with the same condition (W.H.L._90°C_0min) showed an endothermic peak due to water vaporization.

Increasing the duration of the isothermal condition provided enough time for vaporization of water and volatile compounds. Hence, in the second heating, only one step of T_g was observed. T_g was higher for washed samples, due to the removal of small molecules or oligosaccharides, which acted as a plasticizer.

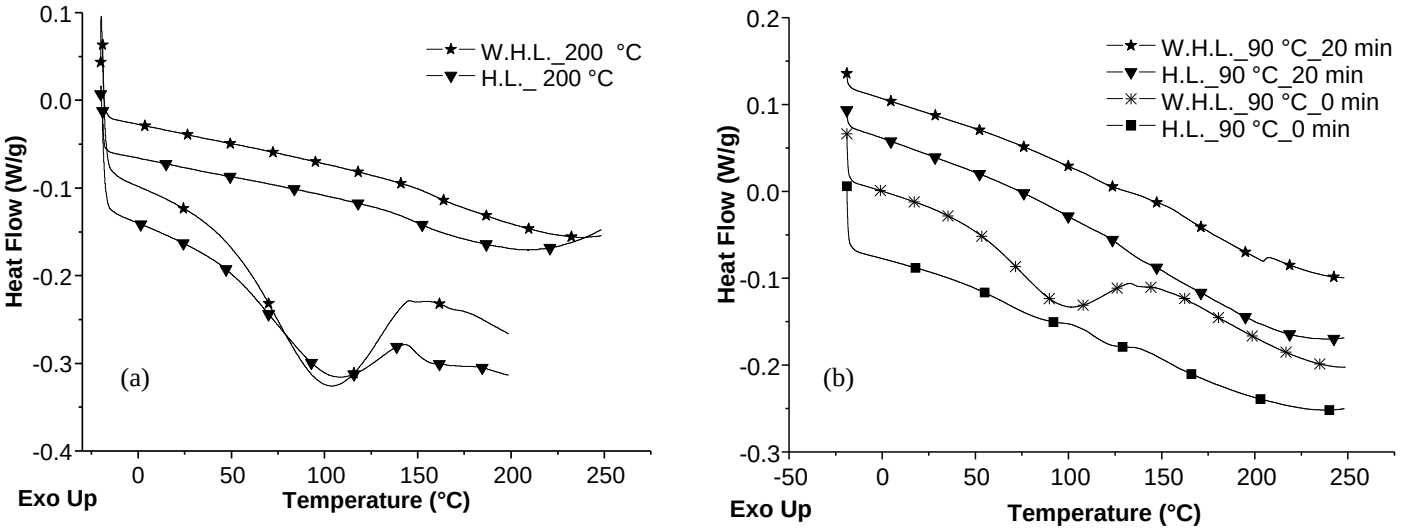

Fig. 5. DSC results of hydrolysis lignin (H.L.) and washed hydrolysis lignin (W.H.L.). a) thermal treatment at 200 °C (Treatment III) (for each sample, the graph for the first heating is below the graph for the second heating), b) thermal treatment at 90 °C at two different isothermal holding time for 0 min and 20 min

In order to separate the reversible and non-reversible thermal events, a temperature-modulated DSC (TMDSC) test was performed. In this experiment, a sinusoidal heat flow was applied to the sample, and reversible and non-reversible heat flows were measured (Fig. 6). Without the need for extra heat-treatment steps to dry the sample, TMDSC enabled glass transition temperature (T_g) measurement from the inflection point on the reversible heat flow or heat capacity graphs, or the maximum of the derivative of reversible heat capacity versus temperature (Guigo *et al.* 2009).

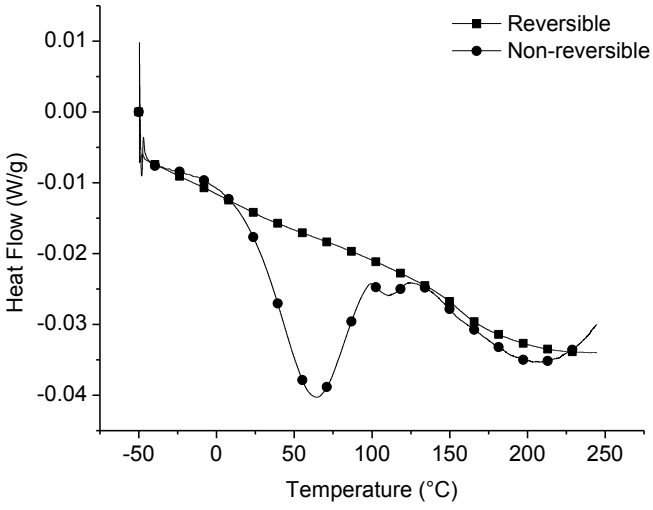

Fig. 6. Temperature-modulated DSC (TMDSC) results of hydrolysis lignin

The T_g obtained from any of these methods was 154 °C for hydrolysis lignin. This T_g value is in agreement with the conventional DSC results after annealing at higher temperature. The non-reversible heat flow graph had peaks at 62 °C and 110 °C. These two temperatures were the same as the two steps prior to the T_g of hydrolysis lignin treated with Treatment I (graph H.L._90°C_0 min in Fig. 5b). This result indicates that the two steps in Fig. 5b were due to non-reversible thermal events. The step at 62 °C nearly disappeared after keeping the hydrolysis lignin at 90 °C for 20 min. As a result, the step at 62 °C cannot be due to the change in molecular conformation or mobility, and may be due to removal of volatile materials which did not have time to move out during the isothermal experiment. A peak at the same temperature as the non-reversible endothermic peak at 110 °C in the TMDSC graph of lignin was also observed as one of the steps before the T_g in the graph for hydrolysis lignin under Treatment I. Since this peak was not apparent for the soluble sample (Fig. 7a), but was apparent for the insoluble fraction (Fig. 7b), it may be due to the carbohydrates or breakage of interactions between lignin and cellulose.

DSC results of soluble and insoluble samples are shown in Fig. 7a and Fig. 7b, respectively. In Fig. 7, all the graphs of treatment under Treatment III display an endothermic peak of water vaporization in the first heating. The maximum temperature of the vaporization peak is lower compared with that of hydrolysis lignin. The water content of the sample can be free or bound to the material. The bound water is restricted by the hydroxyl groups of the natural polymers, cellulose and lignin, and has a different transition temperature than water under standard conditions. The free water in the sample is uninvolved in hydroxyl group bonding (Nakamura *et al.* 1981). The lower temperature of the endothermic peaks of the soluble and insoluble fractions compared with that of hydrolysis lignin suggests that these fractions had less interaction with water than hydrolysis lignin. The level of interaction is due to the distribution of the total lignin and cellulose content of hydrolysis lignin between soluble and insoluble fractions.

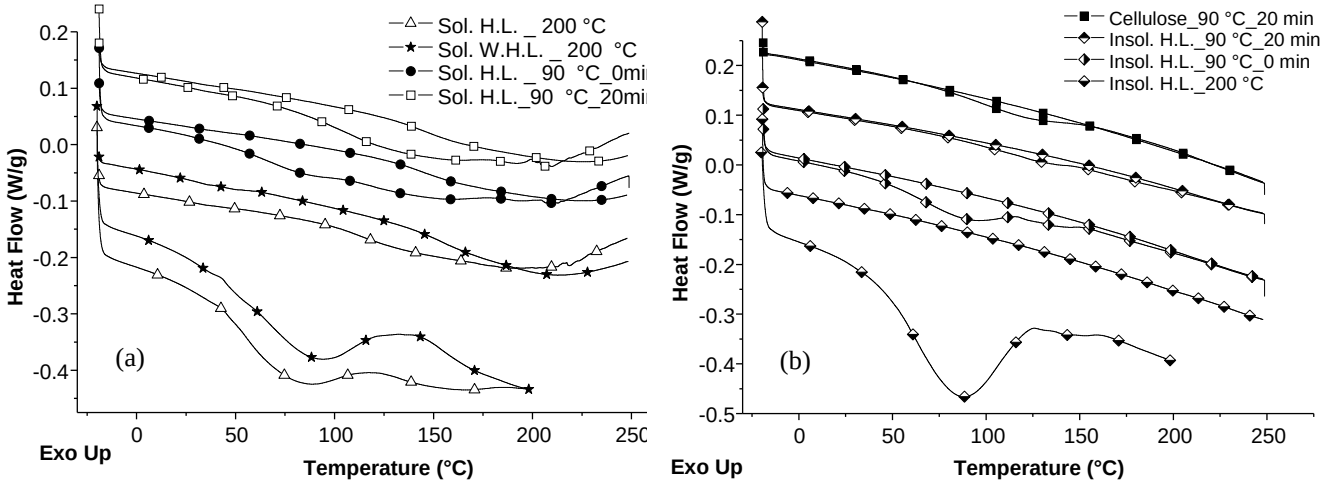

Fig. 7. DSC results of the soluble fraction of hydrolysis lignin (Sol. H.L.), soluble fraction of washed hydrolysis lignin (Sol. W.H.L.), insoluble fraction of hydrolysis lignin (Insol. H.L.), and cellulose. a) soluble samples under Treatments I, II, and III, b) insoluble samples under Treatments I, II, and III (for each sample, the graph for the first heating is below the graph for the second heating)

The T_g of the soluble fraction of hydrolysis lignin and washed hydrolysis lignin, measured from results of Treatment III (thermal treatment at 200 °C), are 112 °C and 154 °C, respectively (Fig. 7a). Both these values are lower than values for hydrolysis lignin and washed hydrolysis lignin. In hydrolysis lignin the presence of crystalline cellulose and the low mobility of its molecules hinder the movement of lignin chains. Washing the material with water increased T_g because the small molecules which can act as a plasticizer are soluble in both water and DMF. Therefore removing them by water prior to dissolving in DMF improves T_g of the soluble fraction. The results of the thermal treatment of the soluble sample at 90 °C, without holding the isothermal condition, exhibited two steps in the first heating after thermal treatment. The sample subjected to 20 min of holding the isothermal condition shows one step. Fig. 7b shows the results of the insoluble sample in comparison with cellulose. The first heating after the thermal treatment has the same trend as the soluble fraction and hydrolysis lignin. However, unlike results from the hydrolysis lignin and the soluble fraction, no step is observed in the second heating. The results after the second heating become similar to cellulose behavior. This sample has a high percentage of carbohydrates and the free movement of lignin molecules is hindered by cellulose molecules. The magnitude of the T_g based on the first heating after holding the isothermal condition at 90 °C for 20 min is 120 °C.

X-ray Diffraction (XRD)

Among the different components available in the hydrolysis lignin, cellulose and lignin have distinct differences in their crystallinity. Cellulose is a crystalline material, while lignin is amorphous. The crystalline segments of cellulose are more resistant to enzymatic hydrolysis (Taherzadeh and Karimi 2007) and thus remain intact in the coproduct of the process. The presence of cellulose in the samples was tracked with XRD analysis. XRD results of hydrolysis lignin and its soluble and insoluble fractions are shown in Fig. 8.

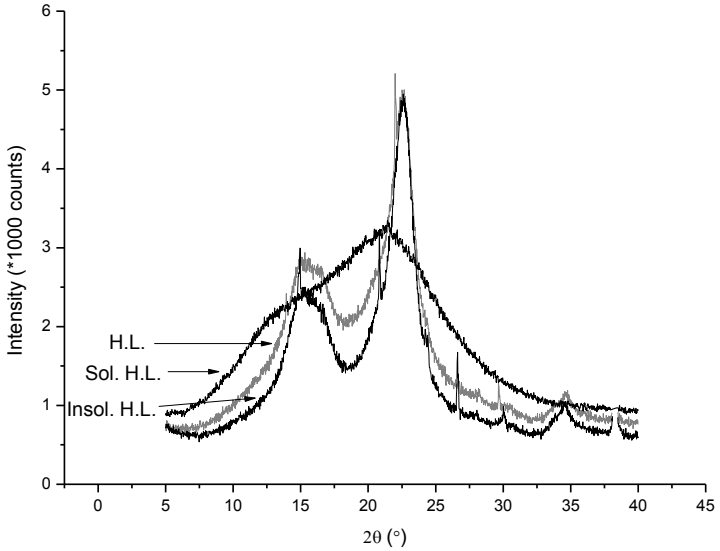

Fig. 8. XRD results of hydrolysis lignin (H.L.) and its soluble (Sol. H.L.) and insoluble (Insol. H.L.) fractions

The hydrolysis lignin and insoluble fraction have three peaks at 2θ = 15, 22.5, and 35. These are due to the $1\bar{1}0$, 110, and 200 crystalline planes of cellulose (Fernández-

Bolaños *et al.* 1999; Paes *et al.* 2010). The soluble sample only shows a broad peak, which is characteristic of amorphous lignin. This technique clearly shows the fractionation of cellulose and lignin between different samples. It also explains the high thermal stability and transition points of the insoluble fraction.

In this study, lignin was extracted from a solid coproduct of cellulosic ethanol industry by solid-liquid extraction. The extracted material and the residue were further analyzed. The rationale behind selecting FTIR, thermal, and XRD experiments is that they are commonly available and require simple sample preparation. The organic solvent (DMF) was used to extract lignin because the solution can be directly used in solution spinning techniques such as electrospinning. The lignin fibers are usually carbonized and properties of the lignin solution affect the processing conditions and the fibers quality. Furthermore, thermal properties of the lignin are important to determine the carbonization conditions. The insoluble residue is a mixture of lignin and carbohydrates which is mainly crystalline cellulose and can be further broken down to extract the cellulose and lignin.

CONCLUSIONS

1. Composition analysis of cellulosic ethanol coproduct, which is the solid residue of an enzymatic hydrolysis of a pretreated biomass (hydrolysis lignin), showed that the hydrolysis lignin contained about 62.5% lignin and the remaining was non-hydrolyzed carbohydrates.
2. N,N- dimethyl formamide (DMF) was used as the solvent for lignin extraction from the bioethanol coproduct. It is an effective solvent for extracting the lignin and also the solution can be used for solution processes such as electrospinning. However, it may be an expensive process for the industrial scale up. Further assessment is required to compare the economics of this process with a two-step extraction and dissolution. The hydrolysis lignin was fractionated into a soluble (lignin-rich fraction) and an insoluble residue with about 43% lignin.
3. The soluble fraction had higher carbon content and lower molecular weight which is consistent with the fact that lignin structure degrades and breaks down during the pretreatment process. The insoluble residue had the highest molecular weight and lowest carbon content. This fraction is made of the more resistant parts of the biomass to the pretreatment and hydrolysis processes. This residue is a mixture of the non-hydrolyzed cellulose, high molecular weight lignin, and lignin–carbohydrate complexes.
4. X-ray diffraction results confirmed the presence of crystalline cellulose in the insoluble residue. Higher crystallinity and molecular weight of this fraction resulted in higher thermal stability and glass transition temperature. In contrast, the high lignin content of the soluble fraction resulted in the higher final residue after thermal degradation.
5. Washing the hydrolysis lignin with water was used to remove the water-soluble compounds and to improve the thermal properties of the hydrolysis lignin and its fractions.

6. In addition to the study of the glass transition points of the hydrolysis lignin by the conventional DSC and different heating cycles, temperature-modulated DSC (TMDSC) was also performed. By using TMDSC the need for extra heating cycles before measuring the transition points was removed. This technique separates the reversible and non-reversible thermal events; therefore it becomes easier and more reliable to recognize the relationship between T_g values and the influence of multiple processing steps due to the material's thermal history or other events such as water vaporization.

ACKNOWLEDGMENTS

The financial support from the Natural Sciences and Engineering Research Council (NSERC), Canada, for the individual Discovery grant (to Misra) and for NSERC NCE AUTO21 to carry out this research is gratefully acknowledged.

REFERENCES CITED

Alvira, P., Tomás-Pejó, E., Ballesteros, M., and Negro, M. J. (2010). "Pretreatment technologies for an efficient bioethanol production process based on enzymatic hydrolysis: A review," *Bioresour. Technol.* 101(13), 4851-4861.

Bjarnestad, S., and Dahlman, O. (2002). "Chemical compositions of hardwood and softwood pulps employing photoacoustic Fourier transform infrared spectroscopy in combination with partial least-squares analysis," *Anal. Chem.* 74(22), 5851-5858.

Bodîrlâu, R., and Teacâ, C. A. (2009). "Fourier transform infrared spectroscopy and thermal analysis of lignocellulose fillers treated with organic anhydrides," *Rom. Journ. Phys.* 54(1-2), 93-104.

Boeriu, C. G., Bravo, D., Gosselink, R. J. A., and van Dam, J. E. G. (2004). "Characterisation of structure-dependent functional properties of lignin with infrared spectroscopy," *Ind. Crop. Prod.* 20(2), 205-218.

Bouajila, J., Dole, P., Joly, C., and Limare, A. (2006). "Some laws of a lignin plasticization," *J. Appl. Polym. Sci.* 102(2), 1445-1451.

Dallmeyer, I., Ko, F., and Kadla, J. F. (2010). "Electrospinning of technical lignins for the production of fibrous networks," *J. Wood Chem. Technol.* 30(4), 315-329.

Doherty, W. O. S., Mousavioun, P., and Fellows, C. M. (2011). "Value-adding to cellulosic ethanol: Lignin polymers," *Ind. Crop. Prod.* 33(2), 259-276.

Fernández-Bolaños, J., Felizón, B., Heredia, A., Guillén, R., and Jiménez, A. (1999). "Characterization of the lignin obtained by alkaline delignification and of the cellulose residue from steam-exploded olive stones," *Bioresour Technol* 68(2), 121-132.

FitzPatrick, M., Champagne, P., Cunningham, M. F., and Whitney, R. A. (2010). "A biorefinery processing perspective: Treatment of lignocellulosic materials for the production of value-added products," *Bioresour. Technol.* 101(23), 8915-8922.

Gellerstedt, G., Sjöholm, E., and Brodin, I. (2010). "The wood-based biorefinery: A source of carbon fiber?" *The Open Agriculture Journal* (www.benthamscience.com), 3, 119-124.

Guigo, N., Mija, A., Vincent, L., and Sbirrazzuoli, N. (2009). "Molecular mobility and relaxation process of isolated lignin studied by multifrequency calorimetric experiments," *Phys. Chem. Chem. Phys.* 11(8), 1227-1236.

Guo, G., Li, S., Wang, L., Ren, S., and Fang, G. (2013). "Separation and characterization of lignin from bio-ethanol production residue," *Bioresour. Technol.* 135, 738-741.

Hansen, C. M. (2000). *Hansen Solubility Parameters : A User's Handbook,* CRC Press, London.

Hatakeyama, H., Tsujimoto, Y., Zarubin, M., Krutov, S., and Hatakeyama, T. (2010). "Thermal decomposition and glass transition of industrial hydrolysis lignin," *J. Therm. Anal. Calorim.* 101(1), 289-295.

Hatakeyama, T., Nakamura, K., and Hatakeyama, H. (1982). "Studies on heat capacity of cellulose and lignin by differential scanning calorimetry," *Polymer* 23(12), 1801-1804.

Holladay, J. E., Bozell, J. J., White, J. F., Johnson, D. (2007). *Top Value-Added Chemicals from Biomass. Volume II—Results of Screening for Potential Candidates from Biorefinery Lignin,* U.S. Department of Energy - Energy Efficiency and Renewable Energy, Pacific Northwest National Laboratory.

Kadla, J. F., Kubo, S., Venditti, R. A., Gilbert, R. D., Compere, A. L., and Griffith, W. (2002). "Lignin-based carbon fibers for composite fiber applications," *Carbon* 40(15), 2913-2920.

Ke, J., Laskar, D. D., and Chen, S. (2011). "Biodegradation of hardwood lignocellulosics by the western poplar clearwing borer, *Paranthrene robiniae* (Hy. Edwards)," *Biomacromolecules* 12(5), 1610-1620.

Kubo, S., and Kadla, J. F. (2005). "Lignin-based carbon fibers: Effect of synthetic polymer blending on fiber properties," *J. Polym. Environ.* 13(2), 97-105.

Kumar, P., Barrett, D. M., Delwiche, M. J., and Stroeve, P. (2009). "Methods for pretreatment of lignocellulosic biomass for efficient hydrolysis and biofuel production," *Ind. Eng. Chem. Res.* 48(8), 3713-3729.

Kumar, R., Hu, F., Sannigrahi, P., Jung, S., Ragauskas, A. J., and Wyman, C. E. (2013). "Carbohydrate derived-pseudo-lignin can retard cellulose biological conversion," *Biotechnol. Bioeng.* 110(3), 737-753.

Li, M. F., Sun, S. N., Xu, F., and Sun, R. C. (2012). "Formic acid based organosolv pulping of bamboo (*Phyllostachys acuta*): Comparative characterization of the dissolved lignins with milled wood lignin," *Chem. Eng. J.* 179, 80-89.

Lisperguer, J., Perez, P., and Urizar, S. (2009). "Structure and thermal properties of lignins: Characterization by infrared spectroscopy and differential scanning calorimetry," *J. Chil. Chem. Soc.* 54(4), 460-463.

Lora, J. H., and Glasser, W. G. (2002). "Recent industrial applications of lignin: a sustainable alternative to nonrenewable materials," *J. Polym. Environ.* 10(1), 39-48.

Lynd, L. R. (1996). "Overview and evaluation of fuel ethanol from cellulosic biomass: technology, economics, the environment, and policy," *Annu. Rev. Energy Environ.* 21(1), 403-465.

Mansouri, N. E., and Salvadó, J. (2006). "Structural characterization of technical lignins for the production of adhesives: Application to lignosulfonate, kraft, soda-anthraquinone, organosolv and ethanol process lignins," *Ind. Crop. Prod.* 24(1), 8-16.

Meunier-Goddik, L., Bothwell, M., Sangseethong, K., Piyachomkwan, K., Chung, Y., Thammasouk, K., Tanjo, D., and Penner, M. H. (1999). "Physicochemical properties of pretreated poplar feedstocks during simultaneous saccharification and fermentation," *Enzyme Microb. Technol.* 24(10), 667-674.

Nakamura, K., Hatakeyama, T., and Hatakeyama, H. (1981). "Studies on bound water of cellulose by differential scanning calorimetry," *Text. Res. J.* 51(9), 607-613.

Paes, S., Sun, S., MacNaughtan, W., Ibbett, R., Ganster, J., Foster, T., and Mitchell, J. (2010). "The glass transition and crystallization of ball milled cellulose," *Cellulose* 17(4), 693-709.

Pan, X., Kadla, J. F., Ehara, K., Gilkes, N., and Saddler, J. N. (2006). "Organosolv ethanol lignin from hybrid poplar as a radical scavenger: Relationship between lignin structure, extraction conditions, and antioxidant activity," *J. Agric. Food Chem.* 54(16), 5806-5813.

Ramos, L. P., Mathias, A. L., Silva, F. T., Cotrim, A. R., Ferraz, A. L., and Chen, C. -. (1999). "Characterization of residual lignin after SO_2-catalyzed steam explosion and enzymatic hydrolysis of *Eucalyptus viminalis* wood chips," *J. Agric. Food Chem.* 47(6), 2295-2302.

Rutkowska, E. W., Wollboldt, P., Zuckerstätter, G., Weber, H. K., and Sixta, H. (2009). "Characterization of structural changes in lignin during continuous batch kraft cooking of *Eucalyptus globulus*," *BioResources* 4(1), 172-193.

Sahoo, S., Seydibeyoğlu, M. Ö., Mohanty, A. K., and Misra, M. (2011). "Characterization of industrial lignins for their utilization in future value added applications," *Biomass Bioenerg.* 35(10), 4230-4237.

Shevchenko, S., Beatson, R., and Saddler, J. (1999). "The nature of lignin from steam explosion/enzymatic hydrolysis of softwood," *Appl. Biochem. Biotechnol.* 79(1-3), 867-876.

Sims, R. E. H., Mabee, W., Saddler, J. N., and Taylor, M. (2010). "An overview of second generation biofuel technologies," *Bioresour. Technol.* 101(6), 1570-1580.

Skrebets, T. E., and Bogolitsyn, K. G. (2009). "Calorimetric study of the interaction between lignin and aprotic solvents," *Russian Journal of Applied Chemistry* 82(2), 228-230.

Sluiter, A., Hames, B., Ruiz, R., Scarlata, C., Sluiter, J., Templeton, D., and Crocker, D. (2008). *Determination of Structural Carbohydrates and Lignin in Biomass. Laboratory Analytical Procedure*, National Renewable Energy Laboratory, U.S. Department of Energy, USA.

Sluiter, A., Hames, B., Ruiz, R., Scarlata, C., Sluiter, J., and Templeton, D. (2005). *Determination of Ash in Biomass. Laboratory Analytical Procedure*, National Renewable Energy Laboratory, U.S. Department of Energy, USA.

Spiridon, I., Teacă, C. A., and Bodîrlău, R. (2011). "Structural changes evidenced by FTIR spectroscopy in cellulosic materials after pre-treatment with ionic liquid and enzymatic hydrolysis," *BioResources* 6(1), 400-413.

Suhas, Carrott, P. J. M., and Carrott, M. M. L. R. (2007). "Lignin - from Natural Adsorbent to Activated Carbon: A Review," *Bioresour. Technol.* 98(12), 2301-2312.

Taherzadeh, M. J., and Karimi, K. (2007). "Enzyme-based hydrolysis processes for ethanol from lignocellulosic materials: A review," *BioResources* 2(4), 707-738.

Thammasouk, K., Tandjo, D., and Penner, M. H. (1997). "Influence of extractives on the analysis of herbaceous biomass," *J. Agric. Food Chem.* 45(2), 437-443.

Article submitted: March 18, 2013; Peer review completed: May 27, 2013; Revised version received and accepted: August 10, 2013; Published: August 19, 2013.